encit 2020

ABCM Associação Brasileira de Engenharia e Ciências Mecânicas

18th Brazilian Congress of Thermal Sciences and Engineering
November 16–20, 2020 (Online)

ENC-2020-0108
TEMPERATURE EFFECT ON MICROSTRUCTURAL ANALYSIS OF STEEL DURING HEAT TREATMENT

Samuel Silva de Brito
Marcos Paulo de Souza Junior
Luiz Carlos Gomes Sacramento Junior
Rodolfo do Lago Sobral
Centro Federal de Educação Tecnológica Celso Suckow da Fonseca - CEFET, Nova Iguaçu, RJ
samuel.brito@aluno.cefet-rj.br
marcos.paulo@aluno.cefet-rj.br
luiz.sacramento@cefet-rj.br
rodolfo.sobral@cefet-rj.br

Abstract. *The present work demonstrates the influence of heat transfer on the evolution of the microstructure of a SAE 1020 carbon steel flat plate. The solution was developed by numerical simulation of the heat transfer equation using the finite difference method and the Crank-Nicolson scheme. The progress of the microstructure is directly related to the mechanical properties of the material, being mainly influenced by temperature. Since the heat transfer in the plate occurs from the edges to the center, the temperatures are higher in the extreme regions, so these regions will have higher temperatures and will reach thermal equilibrium first than the center. Thus, the extreme regions will have more time within the isothermal range, therefore they will have greater evolution of their microstructure and higher rates of recrystallization. The preliminary results show the strong influence of the boundary conditions on the precision of the solution in relation to the expected real model.*

Keywords: *Numerical Simulation, Heat Transfer, Microstructure Evolution, Recrystallization.*

1. INTRODUCTION

Heat treatment processes are used to significantly improve the mechanical properties of the most varied types of steel. A wide variety of engineering projects with enhanced metals are related to the processes of controlling the microstructure of steel, such as annealing, quenching and tempering (Edmonds *et al.*, 2006; Ferguson *et al.*, 2005).

The effective guarantee of the final microstructure of the metals is given by analyzing the microstructure in microscope, however computer simulations are used to predict possible operational failures.

In this work, a SAE 1020 carbon steel flat plate will be placed in a constant temperature furnace for the quenching process. The temperature distribution and its relationship with the phase change of the steel will be studied.

The quenching process consists of heating the steel to a temperature above the critical zone, keeping it at that temperature for a certain time and then cooling it abruptly.

Santofimia *et al.* (2009) experimentally analyzed the microstructure by tempering a low carbon steel, starting with a partial change in the microstructure at a fixed temperature of 900°C and then a rapid cooling in the range of 125°C and 175°C, followed by an isothermal treatment at different intervals of time. Then, the portions of each stage present in multiphase microstructures are measured using optical microscopy and scanning electron microscopy.

Saha *et al.* (2010) empirically presented an annealed carbon steel subjected to cyclic heat treatment process that consisted of repeated short-duration at fixed temperature followed by forced air cooling. After 8 cycles the microstructure mostly contained fine ferrite grains and spheroidized cementite.

Ozisik (1993) showed the temperature distribution according to the finite difference method, time dependent, and unconditionaly stable through the Crank-Nicolson scheme.

Laasraoui and JJ (1991) studied heat transfer during the hot rolling process on steel to determine the flow tension and microstructure. Showing the possibility to predict the microstructure of material through of temperature distribution.

Jang *et al.* (2000) carried out its study by numerical results of the heat transfer, using the finite element method to use the temperature distribution to investigate the microstructure evolution of the material in the hot forging process. In order to demonstrate the validity of the study, the results from the simulation were compared with those of the experiment made.

Shen *et al.* (2018) propose a modification of the Avrami recrystallization model, for the Nb-V microalloyed steel,

in order to get closer to the data found experimentally. With experiments and numerical simulation, the comparison of results shows that the modified model can accurately describe the reality of the process.

Hadadzadeh *et al.* (2018) studied dynamic recrystallization of a molten homogenized ZK60 magnesium alloy. With the temperature set at $400°$C and $450°$C a uniaxial load was imposed with three different strain rates. The models used were calibrated and validated for hot deformation of the alloy, and compared to find out which and in which range the models can be used successfully.

In a complementary way, Alvarado-Juárez *et al.* (2020) presents a comparative numerical and analytical study of heat transfer and how the numerical study can well represent the process nature. And Chen *et al.* (2018) experimentally analyzes the consequences of heat transfer on the surface of ceramic materials.

As can be seen, there are many studies on numerical analysis of heat transfer, and an even greater variety in studies of the mechanical properties of materials, this second, most of which are done in a practical way. In this study, these two characteristics mentioned above will be combined to promote an analysis of the material's attributes, when influenced by temperature, through numerical modeling of heat exchange, based on existing analytical models.

The objective of the work is to relate the heat transfer and the recrystallization equation of the flat steel plate to discover the relationship between the time the plate is heated and the percentage of local recrystallization. The heat transfer solution related to the Avrami equation considered the microstructural evolution over time. An analysis of the finite difference method was performed, using thermal and mechanical properties obtained in thermodynamic calculations and in the classical literature.

2. MATHEMATICAL MODELS

This section aims to expose the theoretical modeling that will be used in the generation and analysis of the results that will be exposed later.

2.1 Heat transfer equation

In the present work, there is no heat generation and the conduction is two-dimensional. The model is based on the partial differential equation of heat, according to (Ozisik, 1993) where the variables t, T and α represents time, temperature and thermal diffusivity respectively. Considering the isotropic material the equation is:

$$\frac{\partial T}{\partial t} = \alpha \left[\frac{\partial^2 T}{\partial x^2} + \frac{\partial^2 T}{\partial y^2} \right], \qquad where \quad \alpha = \frac{k}{\rho\, c} \quad (m^2/s) \tag{1}$$

Where variables k, ρ and c represent thermal conductivity, density and specific heat capacity in that order.

2.2 Finite difference method

The finite difference method consists of reformulating the differential equations so that the derivatives constitute finite intervals instead of infinitesimals. Truncating the Taylor series finite differences are obtained. The variables x and y represent the axes i, j and n are counting variables. The following approximations will be used.

First order forward.

$$\left\langle \frac{\partial T}{\partial t} \right\rangle_{i,j}^{n} \approx \frac{T_{i,j}^{n+1} - T_{i,j}^{n}}{\Delta t} \tag{2}$$

$$\left\langle \frac{\partial T}{\partial x} \right\rangle_{i,j}^{n} \approx \frac{T_{i+1,j}^{n} - T_{i,j}^{n}}{\Delta x} \tag{3}$$

First order backward.

$$\left\langle \frac{\partial T}{\partial x} \right\rangle_{i,j}^{n} \approx \frac{T_{i,j}^{n} - T_{i-1,j}^{n}}{\Delta x} \tag{4}$$

Second order central.

$$\left\langle \frac{\partial^2 T}{\partial x^2} \right\rangle_{i,j}^{n} \approx \frac{T_{i-1,j}^{n} - 2\,T_{i,j}^{n} + T_{i+1,j}^{n}}{\Delta x^2} \tag{5}$$

Derivatives for the y axis are analogous to the x axis.

2.3 Crank-Nicolson method

The Crank-Nicolson method is unconditionally stable, unlike conventional methods where there is a limitation for the spatial discretization (Δx, Δy) and time step (Δt), this method ensures stability to the system without imposing any restrictions on them.

However, the method only guarantees the existence of a final solution, it does not guarantee that this solution is physically correct, which is demonstrated in (Patankar and Baliga, 1978). The application of the method for a generic axis w is:

$$\left\langle \frac{\partial^2 T}{\partial w^2} \right\rangle_{i,j}^{n} \approx \frac{1}{2} \left(\frac{T_{i-1,j}^{n} - 2\,T_{i,j}^{n} + T_{i+1,j}^{n}}{\Delta w^2} + \frac{T_{i-1,j}^{n+1} - 2\,T_{i,j}^{n+1} + T_{i+1,j}^{n+1}}{\Delta w^2} \right) \tag{6}$$

2.4 Boundary conditions

At the ends of the geometry there are convective boundary conditions, which can be represented through the diagram shown below.

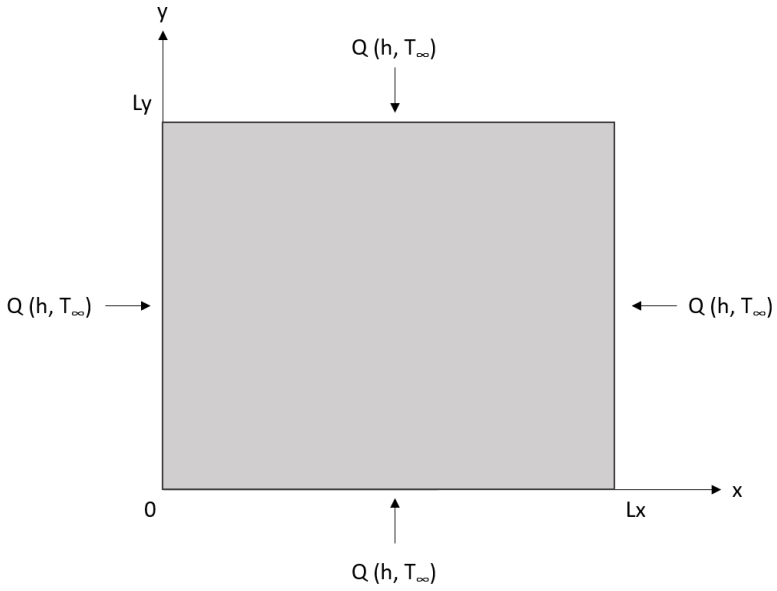

Figure 1. Schematic representation of geometry

Applying the Eq. (2, 6) in (1), the equation that governs the temperature distribution inside the plate according to the numerical model is exposed. And at the edges of the geometry there are.

$$-k\frac{\partial T}{\partial x} = h(T_\infty - T) \qquad for \qquad x = 0 \tag{7}$$

$$k\frac{\partial T}{\partial x} = h(T_\infty - T) \qquad for \qquad x = L_x \tag{8}$$

$$-k\frac{\partial T}{\partial y} = h(T_\infty - T) \qquad for \qquad y = 0 \tag{9}$$

$$k\frac{\partial T}{\partial y} = h(T_\infty - T) \qquad for \qquad y = L_y \tag{10}$$

In this section L_x is the length, L_y the width, h the convective heat transfer coefficient and T_∞ is the reference temperature. Replacing Eq. (3) in (7), and Eq. (4) in (8) and repeating the process for Eq. (9) and (10) the numerical boundary conditions are displayed.

2.5 Initial condition

It is known that at any time the temperature will be between the initial plate temperature and the furnace temperature, both known. Thus, any value between these known temperatures is a possible value for the plate temperature during

the process, so any value between these extreme temperatures is acceptable as a starting value for the simulation. The algorithm will correct the temperature to the expected value using the heat equation. That said, for the start of the simulation, the initial temperature of the plate will be assigned for all time periods.

2.6 Recrystallization rate

AISI 1020 Carbon Steel is classified as hypoeutectoid steel as it has a carbon concentration below 0.8%. The main properties are high ductility, good weldability and low mechanical resistance. The representative microstructure of this steel, when cooled slowly, consists of ferrite and primary perlite. Thus, from the austenite phase it is possible to obtain a percentage amount of austenite transformed into perlite, considering an abrupt cooling of the piece. An equation that translates the recrystallization rates according to (Callister, 2000).

$$x = 1 - exp[-(Kt^{'})^{n^{'}}], \qquad where \quad K = K_0\, exp\left[\frac{-E_c}{RT}\right] \tag{11}$$

Where $t^{'}$ is the effective time, $n^{'}$ is the exponent of Avrami and K is a variable dependent on the Arrhenius velocity constant with temperature. K_0 is the frequency factor, E_c is the activation energy, R the universal gas constant and T the temperature that the process happens. Equation (11) is named as the Avrami equation, as this kinetic model was developed by Johnson-Mehl-Avrami-Kolmogorov (JMAK). The values K_0, $n^{'}$ and E_c were obtained experimentally by (Vieira, 2017) and are shown below.

Table 1. Experimental data

Variable	Value
K_0	3.469·10^6 s^{-1}
E_c	122.69·10^3 $\frac{J}{mol}$
$n^{'}$	0.446

3. MATERIAL DESCRIPTION

Regarding the convective heat transfer coefficient, it was defined following the one used for the numerical and analytical study portrayed by (Oliveira , 2011). The properties used for the steel in question (SAE 1020) were taken from (Davis *et al.*, 1990). The size adopted for the plate, however, was stipulated to fit in an electric oven specially developed for heat treatment, often using tools such as knives. Therefore it accommodates objects with small dimensions.

Table 2. Material and geometrical properties

Parameters	Symbol	Value
Thermal conductivity coefficient	k	51.9 W/(mK)
Density	ρ	7870 kg/m^3
Specific heat capacity	c	486 J/(kgK)
Convective heat transfer coefficient	h	350 W/m^{2}K
Length	L_x	0.1 m
Width	L_y	0.1 m

It is still necessary to define some other parameters for the solution. As can be seen in the iron carbon phase diagram exposed in (Callister, 2000) for the phase change to occur, the temperature must be greater than $727°$C (1000.15 K). Looking again at the iron carbon phase diagram, it is possible to define a temperature, within a range, to heat the plate that will generate the transformation in the austenite phase. It is assumed that before the start of the process the plate was at ambient temperature ($25°$C).

To determine the simulation time, the trial and error method was used to generate preliminary results, until a simulation time long enough to ensure that the time required to reach equilibrium condition is displayed.

Finally, the steps for traversing time and space in numerical simulation are defined. Due to the Crank-Nicolson scheme there is no limitation on the value of the steps to be used, because of this, small values were used, generating a finer mesh, which leads to expect less dissipation between the numerical solutions and the physical process.

4. NUMERICAL SOLUTION

With all the simulation parameters already defined, the objective of the numerical solution of the heat equation and its influence on the behavior of the material remains to be exposed. The numerical solution has mainly two objectives,

Table 3. Simulation Data

Parameters	Symbol	Value
Simulation time	t_s	3000 s
Furnace temperature	T_∞	1073.15 K
Steel starting temperature	T_0	298.15 K
Time step	Δt	0.6250 s
Spatial discretization	Δx	0.0050 m
Spatial discretization	Δy	0.0050 m

the first is to establish when it is possible to declare that a steady state condition has been achieved, which is from that moment that the transformation in the crystalline structure of the piece will begin, and the second objective is to show that this time changes to each geometric point of the mesh.

Then it is necessary to determine a criterion to indicate when the steady state condition is reached, due to the asymptotic characteristic of the system, equilibrium is reached when time tends to infinity, but after a certain point, the temperature variation occurs so slowly that stating a constant temperature is valid for the study.

As can be seen in (Lathi, 2006) in the field of signals and systems, in the stability study, it is common to say that the final condition of the system occurs when it reaches 98% of the expected value (which refers to 5 times the time constant). Using this same argument, the time it takes for each point in the mesh to reach 98% of the reference temperature will be located in the numerical solution presented. With this it will be discovered how long after the start of the process the change in the microstructure will begin.

Ultimately, the expected deviation between the result of the numerical simulation in relation to the physical process is mainly due to the heat transfer by radiation, whose effect on the boundary condition was not estimated in the model. Regarding heat transfer by radiation, it is important to note that its influence depends mainly on two factors, namely, high temperatures and the radiation effects of multiple parts in the process simultaneously. To mitigate these effects, the process will be evaluated with only a single part, since high temperatures cannot be avoided when it comes to heat treatment.

5. RESULTS AND DISCUSSION

From the numerical simulation, the temperature values of each point of the mesh are found during the time interval that was determined. To exemplify the idea, in Fig. 2 the temperature is displayed over time at the point located exactly in the center of the plate (blue line) and when that point reached the stability criterion (red circle).

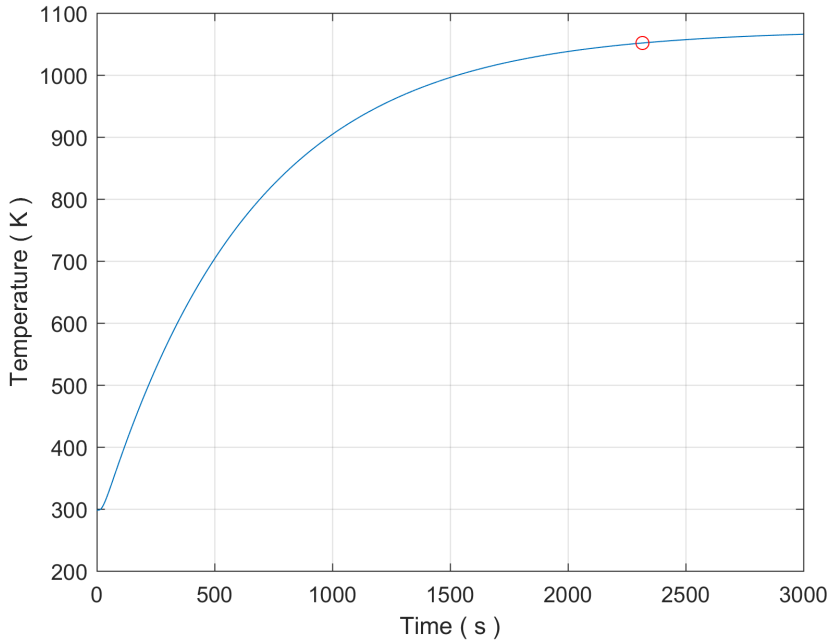

Figure 2. Temperature on the center

Then each point in the mesh will have a curve and a point like the ones shown Fig. 2.

The following Fig.(3) is an outline to interpret the computational domain of the mesh used in the numerical solution. It is appropriate to highlight the size of the mesh in question, which has 21 elements for each of the two axes in question. Due to the nature of the geometry, the mesh in this case can be compared with a matrix of order 21.

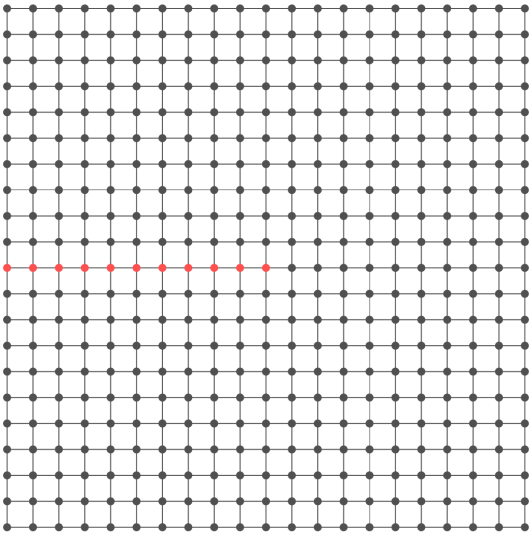

Figure 3. Computational domain

By modeling the heat equation and defining the boundary conditions, it was possible to obtain the time for the plate to reach thermal equilibrium with the furnace, that is, the simulation reaches the steady state. However, it is important to note that the heat transfer in the plate occurs from the edges to the center, that is, the time for the center of the plate to reach thermal equilibrium with the furnace is greater than the edges. Next, these times will be displayed in Table (4)for the points marked in red in Fig. 3.

Since the plate is a flat object that occupies 2 dimensions in space, the computational domain of the mesh coincides with the physical domain of the steel plate.

Table 4. Times to reach steady state condition

Mesh Index	**Time (seconds)**
(11,1)	2269
(11,2)	2278
(11,3)	2286
(11,4)	2293
(11,5)	2299
(11,6)	2304
(11,7)	2308
(11,8)	2312
(11,9)	2314
(11,10)	2316
(11,11)	2316

The index point (11,11) in the mesh is the one that takes the longest to reach equilibrium, which was expected since this point is the one located in the center of the plate.

After this analysis, it was obtained the time that the plate will remain at constant temperature so that the amount of austenite contained in the plate is obtained when it is removed from the oven and cooled down sharply. In order to be able to clearly display the austenitization of the material, a time of 40 minutes was set for the procedure, which will be the time that the plate will be inside the oven, so it is the time that the heat exchange lasts. This time is subtracted from the time it took for the plate to reach the steady state, this subtraction displays the duration of the process of recrystallization of the microstructure, as as previously stated, the phase change only begins after reaching the steady state.

In engineering, most materials are polycrystalline, that is, they are solids formed from an infinity of crystals, called grains. Grain size is an important factor in evaluating the mechanical properties of a material. After a heat treatment,

grain growth tends to occur, however the excessive increase can lead to loss of mechanical properties, since small grains have a larger total area of contours which makes their movement difficult. So, an accurate control when doing the heat treatment, even if aiming at the recrystallization of the material, can prevent the unwanted growth of the grains.

To exemplify the idea exposed above, if the complete recrystallization of the steel plate under study is imposed, however the exact time to reach this purpose is unknown, with prior knowledge of the material in question it is possible to stipulate a very high oven time, which will provide complete recrystallization of the part. However, this exaggerated time would result in an unwanted grain growth, that is, although the goal of 100% recrystallization has been achieved, the mechanical properties may not be positively affected.

Using the Eq. (11), it is possible to obtain the graph for recrystallization rate as shown in Fig. 4.

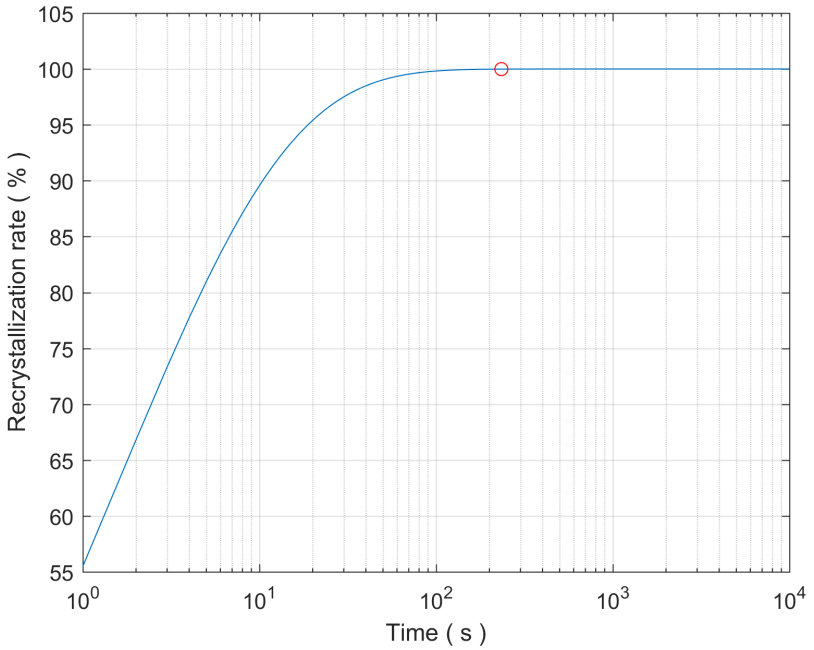

Figure 4. Recrystallization Rate X Time

The red circle represents the point at which the plate reaches 99.99% of the austenite phase, that time is equal to 234 seconds. It is worth mentioning that for the plate to reach 100% austenite, the time would be more than double compared to 99.99%, which would take a very long time to have a much smaller increase than 1%, which was considered a non-significant increase. Once this is done, it is possible to obtain from the Avrami Eq. (11) the recrystallization rate for the entire plate mesh.

Combining the results shown in Fig. (4) and Table (4) it is possible to determine the rate of recrystallization (in percentage) of the points under study (Table 5), these being marked in Fig. (3). These specific points were selected due to the symmetry condition of the plate.

Table 5. Recrystallization rate

Mesh Index	**Recrystallization (%)**
(11,1)	85,66
(11,2)	84,76
(11,3)	83,85
(11,4)	82,99
(11,5)	82,20
(11,6)	81,46
(11,7)	80,84
(11,8)	80,30
(11,9)	79,93
(11,10)	79,68
(11,11)	79,61

So, analyzing the table above, you can see that the same piece has different percentages of austenite. That is, a plate

has a percentage of perlite and another of austenite, not being homogeneous. Austenite presents the Face-Centred Cubic Structure (FCC), its main mechanical characteristics are high wear resistance, ductility, it is a denser component of steels and is not attacked by reagents. Perlite is composed of the Body-Centered Cubic Structure (BCC), presenting less wear resistance and ductility than austenite.

Therefore, for the result obtained from the percentage of austenite previously exposed, we can highlight that the outer surface of the plate for the conditions studied, as it presents a high concentration of austenite, would have a greater hardness than the center. In this sense, a good application for this would be components that need to resist great wear on the external surfaces and little in the center, such as gears.

6. CONCLUSIONS

The control of mechanical properties through the quenching process is directly dependent on several characteristics, such as heating in the temperature range in the austenitic field, grain growth, cooling speed and also post-heat treatment processes, such as tempering, which is essential for remove the brittleness of the material that has just acquired hardness. It is noticed that a procedure that has an objective related to the rate of recrystallization is involved and has consequences and dependence on many others.

The computational modeling of the heat equation on the flat plate, aims to show the temperature distribution in space and time, so that the change in the microstructure of each point can be individually analyzed and present different mechanical properties in the same part. In addition, it is shown that the control of mechanical properties is not an isolated or single procedure, it is the joining of more than one procedure that most of the time is done in more than one step.

Therefore, the correct modeling of the phenomenon of heat transfer and its precise computational model can contribute effectively to avoid possible failures in microstructural control, homogenization and grain size to be targeted for each specific part geometry to be treated.

Finally, in the current configuration, the work developed generates theoretically coherent results. However, for results that are closer to reality, it is necessary to improve mainly the boundary conditions of the heat equation, introducing thermal radiation, which represents a significant portion when working at high temperatures. It is important to note that one of the most frequent experiments for this type of analysis is the Jominy Test, according to (Souza, 2008): "The Jominy test also called the extremity cooling test was developed by Jominy and Boegehold, and is currently one of the most used in industrial practice to assess temperability". That done, the computational modeling can be validated and ready to be incorporated into the heat treatment process on an industrial scale.

7. REFERENCES

Alvarado-Juárez, R., Montiel-González, M., Villafán-Vidales, H., Estrada, C. and Flores-Navarrete, J., 2020. "Experimental and numerical study of conjugate heat transfer in an open square-cavity solar receiver". *International Journal of Thermal Sciences*, Vol. 156, p. 106458.

Callister, W., 2000. *Ciência E Engenharia de Materiais: Uma Introdução* . Grupo Gen-LTC.

Chen, L., Wang, A., Suo, X., Hu, P., Zhang, X. and Zhang, Z., 2018. "Effect of surface heat transfer coefficient gradient on thermal shock failure of ceramic materials under rapid cooling condition". *Ceramics International*, Vol. 44, No. 8, pp. 8992–8999.

Davis, J., Mills, K. and Lampman, S., 1990. "Metals handbook. vol. 1. properties and selection: irons, steels, and high-performance alloys". *ASM International, Materials Park, Ohio 44073, USA, 1990. 1063*.

Edmonds, D., He, K., Rizzo, F., De Cooman, B., Matlock, D. and Speer, J., 2006. "Quenching and partitioning martensite—a novel steel heat treatment". *Materials Science and Engineering: A*, Vol. 438, pp. 25–34.

Ferguson, B.L., Li, Z. and Freborg, A., 2005. "Modeling heat treatment of steel parts". *Computational Materials Science*, Vol. 34, No. 3, pp. 274–281.

Hadadzadeh, A., Mokdad, F., Wells, M. and Chen, D., 2018. "Modeling dynamic recrystallization during hot deformation of a cast-homogenized mg-zn-zr alloy". *Materials Science and Engineering: A*, Vol. 720, pp. 180–188.

Jang, Y.S., Ko, D.C. and Kim, B.M., 2000. "Application of the finite element method to predict microstructure evolution in the hot forging of steel". *Journal of Materials Processing Technology*, Vol. 101, No. 1-3, pp. 85–94.

Laasraoui, A. and JJ, J., 1991. "Prediction of temperature distribution, flow stress and microstructure during the multipass hot rolling of steel plate and strip". *ISIJ international*, Vol. 31, No. 1, pp. 95–105.

Lathi, B.P., 2006. *Sinais e Sistemas Lineares-2*. Bookman.

Oliveira, M.M.P. *et al.*, 2011. "Tratamento térmico de matrizes em aço, estudo do seu aquecimento por convecção/radiação". Dissertação de Mestrado Integrado em Engenharia Mecânica, Universidade do Porto, Faculdade de Engenharia, 71 f.

Ozisik, M.N., 1993. *Heat conduction*. John Wiley & Sons.

Patankar, S. and Baliga, B., 1978. "A new finite-difference scheme for parabolic differential equations". *Numerical Heat Transfer*, Vol. 1, No. 1, pp. 27–37.

Saha, A., Mondal, D.K. and Maity, J., 2010. "Effect of cyclic heat treatment on microstructure and mechanical properties of 0.6 wt% carbon steel". *Materials Science and Engineering: A*, Vol. 527, No. 16-17, pp. 4001–4007.

Santofimia, M., Zhao, L. and Sietsma, J., 2009. "Microstructural evolution of a low-carbon steel during application of quenching and partitioning heat treatments after partial austenitization". *Metallurgical and Materials Transactions A*, Vol. 40, No. 1, p. 46.

Shen, W., Zhang, C., Zhang, L., Xu, Q., Cui, Y. and Xu, Y., 2018. "A modified Avrami equation for kinetics of static recrystallization of nb-v microalloyed steel: Experiments and numerical simulation". *Vacuum*, Vol. 150, pp. 116–123.

Souza, D.A.d., 2008. "Análise da dureza e microestrutura formada após ensaio de temperabilidade Jominy". *Anuário da Produção de Iniciação Científica Discente. Valinhos, SP, Brasil. Anhanguera Educacional S.A.*, Vol. XI, No. 12, p. 735-752.

Vieira, F.S., 2017. "Análise da equação de JMAK no modelamento da formação de austenita para aços hipoeutetóides e hipereutetóides em um processo de aquecimento isócrono". Trabalho de conclusão de curso em Engenharia Mecânica, Universidade Estadual Paulista, Faculdade de Engenharia de Guaratinguetá, 48 f.

8. RESPONSIBILITY NOTICE

The authors are solely responsible for the printed material included in this paper.